Monatshefte für Chemie 129, 975–984 (1998)

Monatshefte für Chemie
Chemical Monthly

Printed in Austria

Synthesis and Characterization of a Novel Dodecanuclear Porphyrin Ruthenium Cluster

Henrique E. Toma*, **Koiti Araki,** and **Edegar O. Silva**

Instituto de Química, Universidade de São Paulo, São Paulo, Brazil

Summary. A new symmetric dodecanuclear complex constituted by a 5,10,15,20-tetra pyridyl porphyrin centre coordinated to four triangular μ-oxo-ruthenium acetate clusters, $[Ru_3O(Ac)_6(py)_2]^+$ (py = pyridine), is reported. Its electrochemical and spectroelectrochemical behaviour involves five accessible oxidation states of the cluster unities, in addition to the porphyrin oxidation and reduction waves, in the range of -1.5 to $+2.4$ V. The cluster porphyrin species associates very strongly with tetrasulfonate phthalocyaninatecopper (II), forming electrostatically assembled stacked compounds both in dimethylsulfoxide solution and in the solid state.

Keywords. Porphyrin cluster; Ruthenium cluster; Supramolecular complex; Spectroelectrochemistry; Electrochemistry.

Synthese und Charakterisierung eines neuen dodekanuklearen Porphyrin-Ruthenium-Clusters

Zusammenfassung. Ein neuer dodekanuklearer Komplex, der durch Koordination eines 5,10,15,20-Tetrapyridylporphyrins an drei dreieckige μ-Oxo-rutheniumacetatcluster ($[Ru_3O(Ac)_6(py)_2]^+$, py = Pyridin) entsteht, wird vorgestellt. Sein elektrochemisches und spektroelektrochemisches Verhalten zeigt, daß im Bereich von -1.5 bis $+2.4$ V zusätzlich zu den Oxidations- und Reduktionswellen des Porphyrins fünf Oxidationszustände der Clustereinheiten zugänglich sind. Der Cluster assoziiert sehr stark mit Tetrasulfonat-phthalocyaninatkupfer(II) und bildet sowohl in Dimethylsulfoxid als auch im festen Zustand elektrostatisch stabilisierte Schichtverbindungen

Introduction

Molecular assemblies of species exhibiting complementary properties are of great interest as models of biological catalysts [1–11] and in studies focusing on electron transfer, artificial photosynthesis [9–15], and molecular devices [4, 16–18]. In this regard, porphyrins and metalloporphyrins are very attractive species for supramolecular design because of their well known catalytic [2, 3, 6, 7, 11, 19] and photochemical [9, 13, 15, 20] properties. Additionally, redox groups can be attached to the porphyrin subunit or at its neighborhood [2, 7, 21–26] in order to explore their complementary role as electron carriers, as in the case of photosynthesis and many biological processes.

*Corresponding author

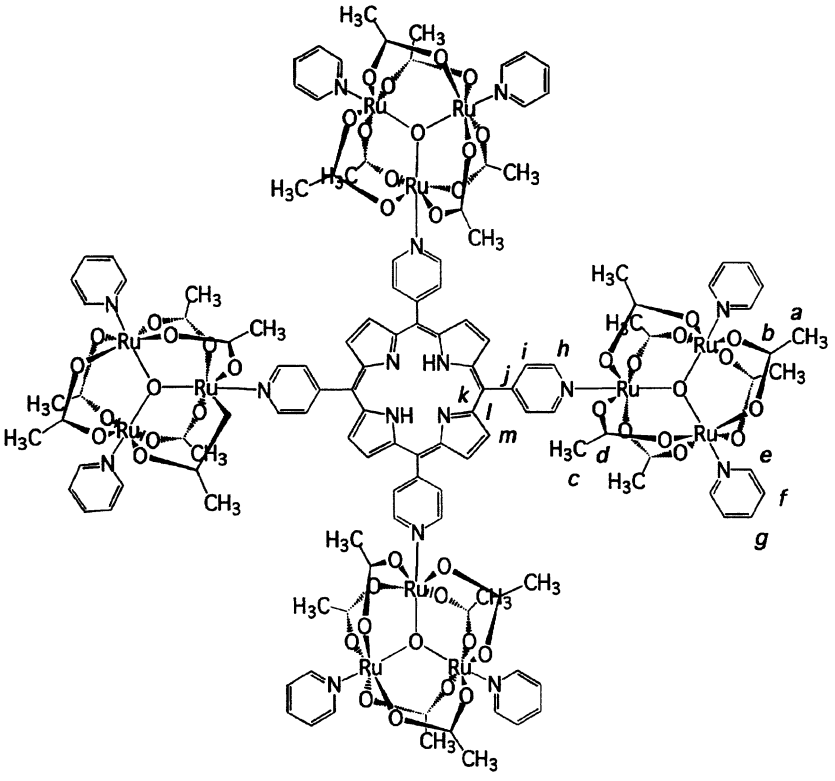

Fig. 1. Structure of the tetracluster porphyrin (*TCP*) supermolecule

In the present work we describe a novel supramolecular species (Fig. 1) consisting of four triangular μ-oxo-ruthenium clusters symmetrically bound to the corners of a square formed by the bidimensional multi-bridging ligand *meso*-tetrapyridylporphyrin (*TPyP*). This species is the prototype of a series of potentially useful redox catalysts, containing a transition metal ion in the porphyrin centre. Although as a free base porphyrin it is not appropriate for catalysis, its synthesis and characterization was pursued with special interest as a starting point for planning and developing the chemistry of this series of supramolecular complexes.

Results and Discussion

^{1}H and ^{13}C NMR

The tetracluster porphyrin is quite stable in the solid state; however, suitable crystals for X-ray analysis have not been obtained up to the present time. For this reason, its structural characterization was conducted by means of ^{1}H and ^{13}C NMR spectroscopy.

The assignment of the ^{1}H and ^{13}C NMR spectra of the *TCP* complex was facilitated by the high symmetry of the molecule which makes all related peripheral cluster resonances equivalent, and was performed by comparison with

the spectra of $[Ru_3O(Ac)_6L_3]^+$ complexes and substituted porphyrins. [27–29]. In the discussion below, the numbering of the H and C atoms will refer to the labels used in Fig. 1.

Two strong singlet observed in the ^{1}H NMR spectrum at 4.49 (48 H) and 4.57 (24 H) ppm were assigned to the H_c and H_a methyl protons of the acetate groups, respectively, based on their intensities and by comparison with the methyl resonances observed for the pyridine cluster [28]. The paramagnetic Ru_3O core is known to induce a large upfield shift on the resonances of the neighboring atoms, supporting the assignment of the peaks at 0.03 (16 H) and 0.73 (8 H) ppm to the H_h and H_e protons of the terminal and bridging pyridine groups. The resonance of the bridging pyridyl group was located at lower field because of the additional porphyrin ring current effect. A resonance peak at 6.13 (16 H) ppm was assigned to the H_f protons, based on its relative intensity and by comparison with the chemical shift observed for the pyridine cluster [28]. The peaks corresponding to the pyridine H_g protons appeared superimposed to those for the H_i protons of the bridging group at 6.63 (8 H) and 6.52 (8 H) ppm. The remaining peaks observed at 7.78 (8 H) ppm and −4.0 (2 H) ppm were straightforwardly assigned to the H_m and N-H protons of the porphyrin centre, respectively [29].

The assignment of the ^{13}C NMR spectrum was performed in a similar way by comparison with the literature [29] and taking into account the upfield shifts induced by the paramagnetic anisotropy of the ruthenium clusters on the nearby carbons. The DEPT spectrum was also recorded in order to facilitate the assignment of the carbon resonances. The proposed assignment is as follows: C_c, −3.5; C_a, −2.9; C_e, 113.8; C_h, 115.0; C_f, 119.3; C_k, 124.3; C_m, 126.4; C_g, 131.5; C_i, 138.3; C_j, 144.0; C_l, 148.8; C_d, 199.2; and C_b 203.2 ppm.

Electrochemistry

The cyclic voltammograms of the *TCP* complex are dominated by the peaks of the μ-oxo-ruthenium acetate cluster moieties, exhibiting four intense waves in the 2.4 to −1.5 V region. The electronic structure of the triangular clusters is typically delocalized: the successive redox waves split by more than 1 V. The waves at 2.3, 1.23, 0.16, and −1.14 V were assigned to successive redox couples, formally represented as $Ru^{IV}Ru^{IV}Ru^{III}/Ru^{IV}Ru^{III}Ru^{III}/Ru^{III}Ru^{III}Ru^{III}/Ru^{III}Ru^{III}Ru^{II}/Ru^{III}Ru^{II}Ru^{II}$, by comparison with previously reported results [30]. Except for the wave at 2.3 V which is near the limit of working potential, the remaining clusters waves were typically reversible, showing two almost symmetric anodic-cathodic peaks separated by 60–75 mV and a linear dependence of the current on the concentration and on the square root of the scan rates. The lack of splittings for the respective cluster waves indicates that the four peripheral unities behave as independent redox sites, *i.e.* the cluster-cluster electronic coupling through the porphyrin bridge is negligible [2, 15, 31].

The porphyrin subunit is also electrochemically active, but the wave intensities should be four times smaller than the waves associated with the ruthenium cluster subunits. In the voltammograms of Fig. 2, the waves at −0.72, −1.05, and 1.68 V present such characteristics and were respectively assigned to the first and second reduction steps and to the oxidation of the porphyrin ring. In contrast to the wave at

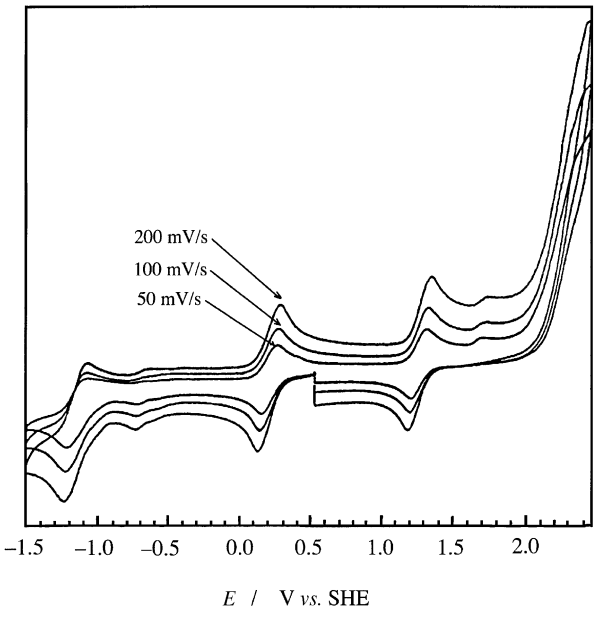

Fig. 2. Cyclic voltammograms of the tetracluster porphyrin complex in acetonitrile, *TEA*ClO_4 0.1 *M*, at different scan rates in the −1.5 to 2.4 V range

−0.72 V which was typically reversible when scanned in isolation, the redox wave at 1.68 V remained very similar to that shown in Fig. 2, suggesting the occurrence of an irreversible process after the oxidation of the porphyrin ring. The second reduction of the porphyrin is evidenced by a shoulder at −1.0 V near the strong reduction wave of the cluster unities at −1.2 V in Fig. 2. The two reduction waves can be compared with those observed at −0.68 and −0.93 V for the analogous tetrapyridylporphyrin species modified with four $[Ru(bipy)_2Cl]^+$ groups [31]. The small shift (∼50 mV) to more negative potentials is consistent with the backbonding interactions from the $Ru^{III}Ru^{III}Ru^{II}$ clusters which increase the electronic density of the porphyrin centre. It is interesting to note that the electrochemistry of the tetracluster porphyrin (in the −1.5 to 2.4 V range) involves a total of 19 electrons, a rather unusual characteristic in transition metal chemistry.

Spectroelectrochemistry

The electronic spectrum of *TCP* in acetonitrile (Fig. 3) exhibits a continuous envelope of superimposed bands from 200 to 800 nm which reflects the presence of the ruthenium clusters and the porphyrin components in the supermolecule. The *Soret* or B band is well defined at 414 nm ($\varepsilon = 2.6\times10^5\ M^{-1}\cdot cm^{-1}$) and is followed by a high energy vibronic shoulder at 382 nm ascribed to the B_{1-0} transition. *Gaussian* functions (calculated by Grams/386 IBM/PC software) and a suitable guess for the number of transitions and their respective energies, obtained by comparison with the spectra of both components, were used to fit the spectrum of the *TCP* supermolecule. The deconvolution was carried out in order to extract the four relatively narrow Q bands at 518, 552, 579, and 645 nm, characteristic of the

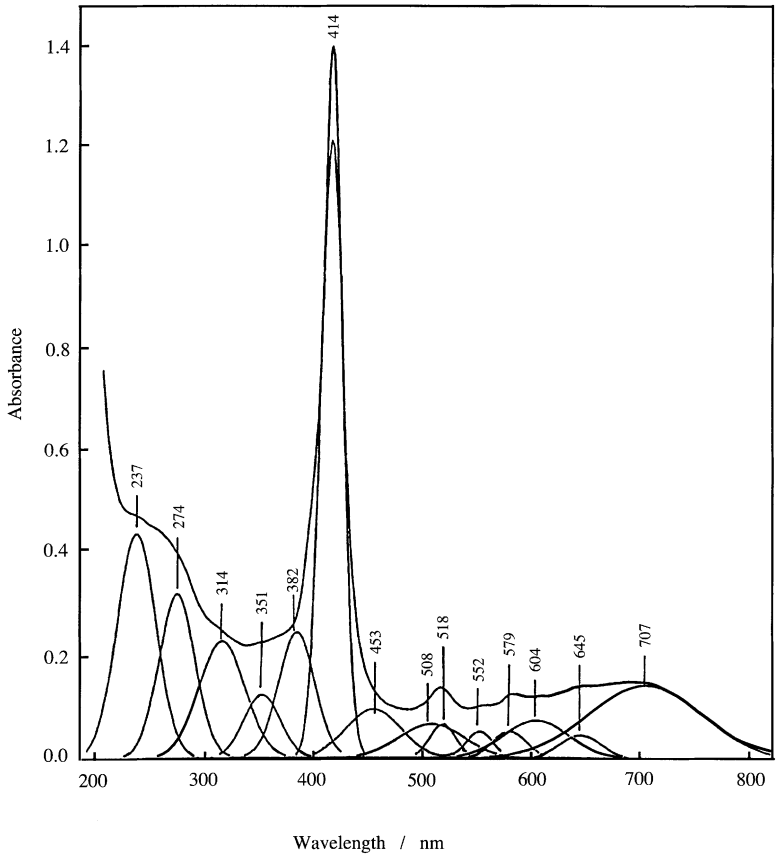

Fig. 3. Electronic spectrum of the porphyrin cluster in acetonitrile solution ($10^{-5}\,M$) and the corresponding *Gaussian* component obtained by spectral deconvolution using the Grams/386 IBM/PC software

porphyrin free-base centre, and the typically broad intracluster bands at 707, 604, and 508 nm (Fig. 3). These results are in complete harmony with the literature spectra of porphyrins and $[Ru_3O(Ac)_6(py)_3]^+$ species [32]. In the ultraviolet region, the absorption bands at 237 and 274 nm can be attributed to $\pi \rightarrow \pi^*$ transitions in the terminal and bridging pyridine groups, respectively [28]. The next two bands at 314 and 351 nm are consistent with charge transfer transitions from the metal cluster to the two types of pyridine ligands, as previously observed for $[Ru_3O(Ac)_6(py)_2(py\text{-}R)]^+$ complexes [28]. The *Gaussian* component at 453 nm has been detected in some μ-oxo ruthenium clusters [32], but can also be a new charge transfer transition involving the cluster and the porphyrin groups, analogously to previously reported tetrametallated porphyrins [10, 11, 23].

The spectroelectrochemistry of the tetracluster porphyrin is shown in Fig. 4a. Starting at 0.5 V and stepping the potential to +1.5 V it is possible to oxidize the peripheral clusters from the $Ru^{III}Ru^{III}Ru^{III}$ to the $Ru^{III}Ru^{III}Ru^{IV}$ state. This process is evidenced by the characteristic decrease of the bands around 650 nm and the increase of absorbance at 826 nm [33]. At the same time, the *Soret* band decreased dramatically due to the oxidation of the porphyrin ring at the onset of the oxidation

peak during the waiting time of about two minutes employed for the spectroelectrochemical measurements.

By applying −0.3 V, a reversible reduction of the starting complex to the $Ru^{III}Ru^{III}Ru^{II}$ state (Fig. 4b) can be observed by the decay of the intra-cluster bands around 650 nm and the rise of a characteristic band at 920 nm. Similar spectral changes can also be observed for the 314 and 351 nm bands which decay, whereas the absorption bands at 370 and 460 nm grow up. This behaviour, *i.e.* the bathochromic shift of the bands at 314 and 351 nm after the reduction of the ruthenium ion, is coherent with their assignment to metal cluster-to-ligand charge transfer transitions [33].

Further reduction of the complex (Fig. 4c) at −1.0 V led to a shift of the *Soret* band from 414 to 460 nm and to the appearance of a broad band around 580 nm,

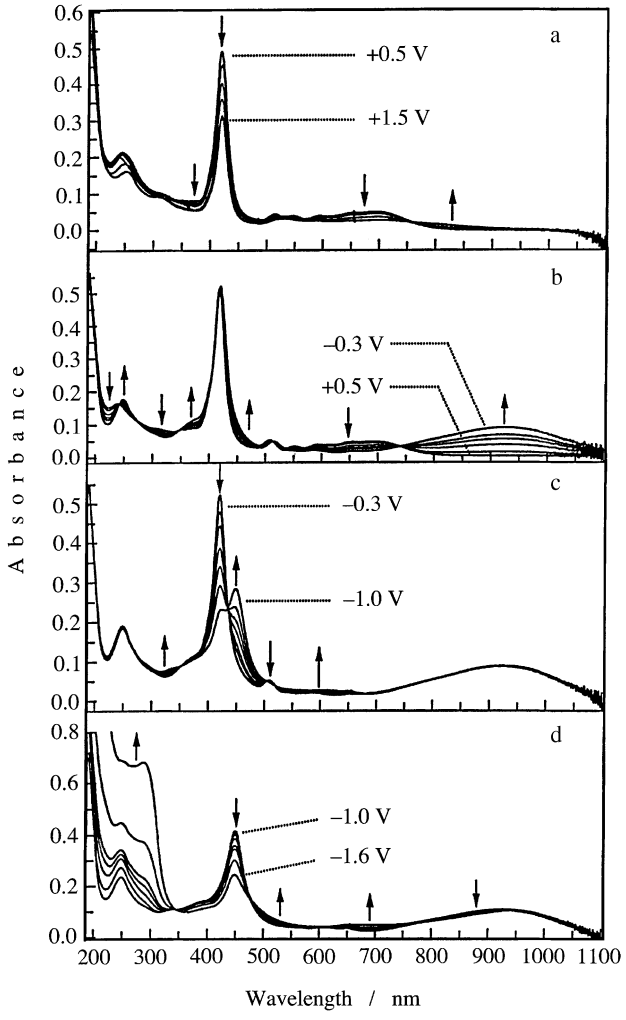

Fig. 4. Spectroelectrochemical behaviour of the tetracluster porphyrin complex in acetonitrile in the range of −1.6 to +1.5 V; the potential ranges for each processes are indicated in the figure; electrolyte: 0.1 *M TEA*ClO_4

whereas the cluster-pyridine bands at 252 and 920 nm remained almost unchanged. In this case, the ruthenium clusters were not affected, but the porphyrin exhibited a spectroelectrochemical behaviour consistent with the conversion of the porphyrin moiety to the radical anion species [23, 31]. Finally, the reduction of the complex at -1.6 V shows the formation of the $Ru^{III}Ru^{II}Ru^{II}$ species (Fig. 4d) leading to a small bathochromic shift of the 920 nm band and to an increased absorbance around 520 nm, ascribed to the ruthenium-to-pyridine MLCT band. In addition, the spectroelectrochemical behaviour of this last reduction wave is dominated by a decrease of the *Soret* band of the porphyrin radical anion, confirming the second reduction process of the porphyrin ring at -1.0 V in the cyclic voltammograms of Fig. 3.

Stacked ion pairs

Porphyrins, phthalocyanines, and related compounds have a strong tendency to associate forming dimers, trimers, and oligomers. This driving force toward association can be enhanced by electrostatic interactions when oppositely charged species are put together [34]. In this case, the formation of stacked ion pairs is strongly favored, as previously reported for $[ZnTPyP(Ru(bipy)_2Cl]_4)^{4+}$ and $[M\text{-}TPPS]^{4-}$, leading to the precipitation of an unsoluble, layered material from methanolic solution [35].

The *TCP* exhibits bulkier peripheral groups than the previously studied polynuclear porphyrins, and the positive charge is delocalized over the triangular μ-oxo(*tris*-ruthenium) core, decreasing the strength of the electrostatic interactions with negatively charged species such as the tetrasulfonate phthalocyaninatecopper (II) (Cu*TSP*c) anion. The titration of a 2.5 μM solution of Cu*TSP*c with a 230 μM solution of *TCP* in *DMSO* is shown in Fig. 5. The addition of *TCP* to the sulfonated copper phthalocyanine solution lead to a decrease of the absorbance of the Q band

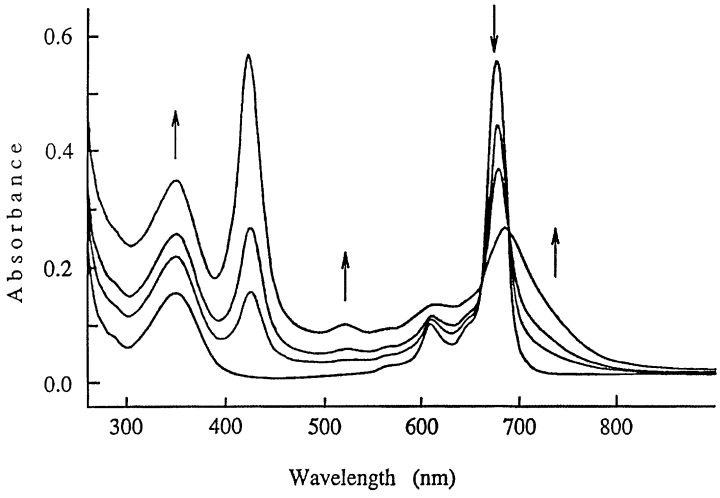

Fig. 5. Titration of a $2.58\times 10^{-6}\,M$ solution of Cu*TSP*c with a $2.29\times 10^{-4}\,M$ solution of *TCP* in *DMSO*; $[TCP]_0/[CuTSPc]_0 = 0.00$, 0.34, 0.56, and 0.99

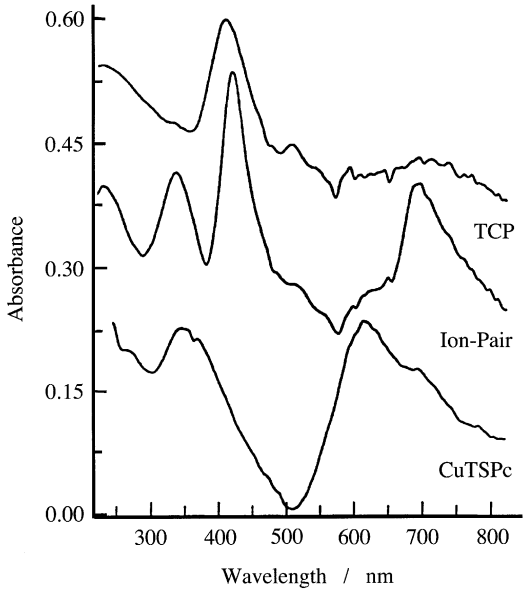

Fig. 6. Reflectance solid state spectrum of *TCP* (top), Cu*TSP*c (bottom), and stacked ion pair (middle) dispersed in MgO

at 677 nm, whereas at other wavelengths an increase was observed due to the absorption of the tetracluster porphyrin. This behaviour is coherent with the formation of a stacked ion pair. A sharp end-point was observed at a 1:1 molar ratio, and two well defined isosbestic points were observed. These results strongly suggest the occurrence of a simple reaction involving Cu*TSP*c, *TCP*, and Cu*TSP*c/*TCP* in which the equilibrium is completely shifted to the right. The ion pair absorbs all over the UV and visible region, but absorption maxima can be observed at 349, 422, 520, 562, 615, and 681 nm. This spectrum is very similar to that obtained at the end-point of the titration of *TCP* with Cu*TSP*c, implying that the same species was formed in both cases.

The stacked species was isolated as a dark solid, and the elemental analysis was coherent with a 1:1 ion pair composition. The absorption spectra of solid *TCP* and Cu*TSP*c (Fig. 6) are broadened because of intermolecular interactions. It should be noted that the Cu*TSP*c is predominantly stacked as evidenced by the blue shifted Q band with a maximum at 615 nm and a shoulder at 694 nm. The solid obtained after mixing the solutions of *TCP* and Cu*TSP*c exhibits sharper bands than the starting species at 232, 336, 417, 516, 621, and 690 nm. This spectrum is clearly very similar to the spectrum of the 1:1 stacked ion pair in *DMSO* solution, suggesting the existence of well defined stacked ion pairs in the solid state.

Final remarks

The NMR spectra provided a reliable evidence that the molecule studied is highly symmetric and constituted exclusively by tetra pyridyl porphyrin linked to four triangular ruthenium acetate clusters. Partial substitution at the *TPyP* centre can be excluded since it would lead to less symmetric species exhibiting additional peaks

in the NMR spectra. Furthermore, the results are coherent with a molecule in which there is a weak interaction between the subunities, such that they can be considered relatively independent. The *TCP* molecule associates strongly with Cu*TSP*c forming 1:1 ion pairs in *DMSO* solution, and similar interactions prevail even in the solid state. Unfortunately, we have not been successful in the preparation of homogeneous electrostatically assembled *TCP*/Cu*TSP*c films. Further studies exploiting the properties and applications of the tetracluster metalloporphyrins are in progress.

Experimental

The complex was synthesized by the reaction of 0.077 g of *TPyP* (Aldrich) and 0.50 g of $[Ru_3O(Ac)_6(py)_2MeOH](PF_6)$ [36] dissolved in a minimum volume of trifluoroethanol (Aldrich) at room temperature protected from light for twenty hours. The compound was precipitated by addition of 50 cm^3 of diethyl ether. The dark green solid obtained after work-up gave elemental analysis values consistent with the composition shown in Fig. 1: $C_{128}N_{16}H_{138}Ru_{12}O_{52}P_4F_{24}$, exp. (calcd): C 33.45 (33.97), N 4.93 (4.95), H 3.29 (3.07). The infrared spectrum in dominated by the peripheral ruthenium acetate cluster vibrational peaks at 1549(m), 1488(m), 1425(s), 1351(s), 1278(w) 1236(vw), 1217(s), 1192(vw), 1156(w), 1048(m), 1019(w), 946(w), 843(vs), 764(m), 740(w), 686 (vs), 621 (m), and 558 (s) cm^{-1}, but typical porphyrin peaks can also be seen at 1609 (s), 1068(m), 1001(w), 971(m), and 802 (m) cm^{-1} (m = medium, s = strong, w = weak, vw = very weak, vs = very strong).

The solid tetraclusterporphyrin/tetrasulfonate phthalocyaninatocopper (II) (*TCP*/Cu*TSP*c) ion pair was prepared by mixing an acetonitrile solution of *TCP* with an aqueous solution of Cu*TSP*c in stoichiometric amounts. The mixture was kept overnight at room temperature, and the green precipitate was isolated by centrifugation, rinsed with water and diethyl ether, and dried under vacuum. Analysis for $C_{106}H_{198}N_{24}O_{88}S_4CuRu_{12}$: expt · (calcd): C 35.44 (36.47), H 3.78 (3.79), N 6.36 (6.38).

The cyclic voltammetry and spectroelectrochemistry measurements were carried out as described previously [2,15] employing a conventional three electrode system with platinum or gold minigrid working electrodes, respectively. The experiments were performed in acetonitrile using an Ag/Ag^+ 0.01 *M* (*TEA*ClO_4 0.1 *M*) reference electrode. All potentials were corrected to SHE by adding 0.503 V as reported in the literature [37].

The electronic spectra were recorded on Hewlett Packard model 8452A or 8453A diode-array spectrophotometers. ^1H and ^{13}C NMR spectra of the complex were obtained using a Bruker 200 MHz NMR spectrometer; the samples were dissolved in *DMSO*-d_6.

Acknowledgments

The authors gratefully acknowledge financial support from *FAPESP*, *CNPq*, and *PADCT*.

References

[1] Angnes L, Azevedo CMN, Araki K, Toma HE (1996) Anal Chim Acta **329**: 91
[2] Araki K, Angnes L, Azevedo CMN, Toma HE (1995) J Electroanal Chem **397**: 205
[3] Bedioui F, Devynck J, Bied-Charreton C (1995) Acc Chem Res **28**: 30
[4] Gilles-Gonzalez MA, Gonzales G, Perutz MF, Kiger L, Marden MC, Poyart C (1994) Biochemistry **33**: 8067
[5] Jayaraj K, Terner J, Gold A, Roberts DA, Austin RN, Mandon D, Weiss R, Bill E, Müther M, Trautwein AX (1996) Inorg Chem **35**: 1632

[6] Shi C, Anson FC (1994) Inorg Chim Acta **225**: 215
[7] Smith JRL (1994) Metalloporphyrins in Catalytic Oxidations. Dekker, New York
[8] Steiger B, Anson FC (1994) Inorg Chem **33**: 5767
[9] Onuki J, Ribas AV, Medeiros MHG, Araki K, Toma HE, Catalani LH, DiMascio P (1996) Photochem Photobiol **63**: 272
[10] Toma HE, Araki K (1990) J Chem Res 82
[11] Toma HE, Araki K (1991) Inorg Chim Acta **179**: 293
[12] Krishnan V, Batova EE, Shafirovich VY (1994) J Photochem Photobiol **84**: 233
[13] Wasielewski MR (1992) Chem Rev **92**: 435
[14] Bonnett R (1995) Chem Soc Rev 19
[15] Araki K, Toma HE (1994) J Photochem Photobiol **83**: 245
[16] Bernard J, Orrit M, Personov RI, Samoilenko AD (1989) Chem Phys Lett **164**: 377
[17] Gunter MJ, Johnston MR (1992) J Chem Soc Chem Commun 1163
[18] Schaafsma TJ (1995) Solar Energy Materials and Solar Cells **38**: 349
[19] Younathan JN, Wood KS, Meyer TJ (1992) Inorg Chem **31**: 3280
[20] Osuka A, Nakajima S, Okada T, Taniguchi S, Nozaki K, Ohno T, Yamazaki I, Nishimura Y, Mataga N (1996) Angew Chem Int Ed Engl **35**: 92
[21] Anson FC, Shi CN, Steiger B (1997) Acc Chem Res **30**: 437
[22] Steiger B, Anson FC (1997) Inorg Chem **36**: 4138
[23] Araki K, Toma HE (1994) J Chem Res (M) 1501
[24] Collin JP, Dalbavie JO, Heitz V, Sauvage JP, Flamini L, Armaroli N, Balzani V, Barigelletti F, Montanari I (1996) Bull Soc Chim France **133**: 749
[25] Flamigni L, Armaroli N, Barigelletti F, Balzani V, Collin JP, Dalbavie JO, Heitz V, Sauvage JP (1997) J Phys Chem B **101**: 5936
[26] Sessler JL, Capuano VL, Burrell AK (1993) Inorg Chim Acta **204**: 91
[27] Alexiou ADP, Toma HE (1997) J Chem Res (S) 338
[28] Toma HE, Alexiou ADP (1995) J Chem Res (S) 134
[29] Janson TR, Katz JJ (1979) Nuclear Magnetic Resonance Spectroscopy of Diamagnetic Porphyrins. In: Dolphin D (ed) The Porphyrins, vol IV. Academic Press, New York, p 1
[30] Alexiou ADP, Toma HE (1993) J Chem Res (S) 464
[31] Toma HE, Araki K (1993) J Coord Chem **30**: 9
[32] Toma HE, Cunha CJ, Cipriano C (1988) Inorg Chim Acta **154**: 63
[33] Toma HE, Cunha CJ (1989) Can J Chem **67**: 1632
[34] Ojadi E, Selzer R, Linschitz H (1985) J Am Chem Soc **107**: 7783
[35] Araki K, Wagner MJ, Wrighton MS (1996) Langmuir **12**: 5393
[36] Bauman JA, Salmon DJ, Wilson ST, Meyer TJ, Hatfield WE (1978) Inorg Chem **17**: 3342
[37] Kratochvil B, Lorah E, Garber C (1969) Anal Chem **41**: 1793

Received January 9, 1998. Accepted (revised) May 4, 1998